



Provided for non-commercial research and education use.  
Not for reproduction, distribution or commercial use.

Volume A826, Issues 3–4 1 August 2009		ISSN 0375-9474
	<b>NUCLEAR PHYSICS A</b>	
<b>Nuclear and Hadronic Physics</b>		
<small>Journal devoted to the experimental and theoretical study of the fundamental constituents of matter and their interactions. Abstracted/Indexed in: Current Contents: Physical, Chemical &amp; Earth Sciences. Also covered in the abstract and citation database SCOPUS®. Full text available on ScienceDirect®</small>		
<small>Supervisory Editors: G.E. Brown, A. Gal, R. Hayano, J. Jolie, K. Langanke, L. McLerran, M. Soyeur, J. Stachel, M. Thoennessen</small>		
NUCLEAR STRUCTURE AND DYNAMICS	D. Pereira, C.P. Silva, J. Lubian, E.S. Rossi Jr., L.C. Chamon, G.P.A. Nobre and T. Correa <i>Understanding fusion suppression and enhancement in the <math>^{18}\text{O} + ^{36,60,64}\text{Ni}</math> systems</i>	211
	T.R. Routray, J. Nayak and D.N. Basu <i>Cluster radioactivity in very heavy nuclei: a new perspective</i>	223
HADRONIC PHYSICS AND HIGH ENERGY QCD	D. Kharzeev, E. Levin, M. Nardi and K. Tuchin <i><math>J/\psi</math> production in heavy ion collisions and gluon saturation</i>	230
ELECTROWEAK INTERACTIONS	P. Belli, R. Bernabei, F. Cappella, R. Cerulli, F.A. Danevich, B.V. Grinyov, A. Incicchitti, V.V. Kobaychev, V.M. Mokina, S.S. Nagorny, L.L. Nagornaya, S. Nisi, F. Nozzoli, D.V. Poda, D. Prosperi, V.I. Tretyak and S.S. Yurchenko <i>Search for double beta decay of zinc and tungsten with low background <math>\text{ZnWO}_4</math> crystal scintillators</i>	256
Available online at  www.sciencedirect.com		

This article appeared in a journal published by Elsevier. The attached copy is furnished to the author for internal non-commercial research and education use, including for instruction at the authors institution and sharing with colleagues.

Other uses, including reproduction and distribution, or selling or licensing copies, or posting to personal, institutional or third party websites are prohibited.

In most cases authors are permitted to post their version of the article (e.g. in Word or Tex form) to their personal website or institutional repository. Authors requiring further information regarding Elsevier's archiving and manuscript policies are encouraged to visit:

<http://www.elsevier.com/copyright>



ELSEVIER

Available online at [www.sciencedirect.com](http://www.sciencedirect.com)

Nuclear Physics A 826 (2009) 256–273

[www.elsevier.com/locate/nuclphysa](http://www.elsevier.com/locate/nuclphysa)

## Search for double beta decay of zinc and tungsten with low background $\text{ZnWO}_4$ crystal scintillators

P. Belli <sup>a</sup>, R. Bernabei <sup>a,\*</sup>, F. Cappella <sup>b</sup>, R. Cerulli <sup>c</sup>, F.A. Danevich <sup>d</sup>,  
 B.V. Grinyov <sup>e</sup>, A. Incicchitti <sup>b</sup>, V.V. Kobychchev <sup>d</sup>, V.M. Mokina <sup>d</sup>,  
 S.S. Nagorny <sup>d</sup>, L.L. Nagornaya <sup>e</sup>, S. Nisi <sup>c</sup>, F. Nozzoli <sup>a</sup>, D.V. Poda <sup>d</sup>,  
 D. Prosperi <sup>b</sup>, V.I. Tretyak <sup>d</sup>, S.S. Yurchenko <sup>d</sup>

<sup>a</sup> *Dipartimento di Fisica, Università di Roma “Tor Vergata” and INFN, Sezione di Roma Tor Vergata, I-00133 Rome, Italy*

<sup>b</sup> *Dipartimento di Fisica, Università di Roma “La Sapienza” and INFN, Sezione di Roma, I-00185 Rome, Italy*

<sup>c</sup> *INFN, Laboratori Nazionali del Gran Sasso, 67010 Assergi (AQ), Italy*

<sup>d</sup> *Institute for Nuclear Research, MSP 03680 Kyiv, Ukraine*

<sup>e</sup> *Institute for Scintillation Materials, 61001 Kharkiv, Ukraine*

Received 28 April 2009; received in revised form 25 May 2009; accepted 26 May 2009

Available online 2 June 2009

### Abstract

Double beta processes in  $^{64}\text{Zn}$ ,  $^{70}\text{Zn}$ ,  $^{180}\text{W}$ , and  $^{186}\text{W}$  have been searched for with the help of large volume (0.1–0.7 kg) low background  $\text{ZnWO}_4$  crystal scintillators at the Gran Sasso National Laboratories of the INFN (Italy). The total measurement time exceeds ten thousand hours. New improved half-life limits on double electron capture and electron capture with positron emission in  $^{64}\text{Zn}$  have been set, in particular (all the limits are at 90% C.L.):  $T_{1/2}^{0\nu 2\varepsilon} \geq 1.1 \times 10^{20}$  yr,  $T_{1/2}^{2\nu\varepsilon\beta^+} \geq 7.0 \times 10^{20}$  yr, and  $T_{1/2}^{0\nu\varepsilon\beta^+} \geq 4.3 \times 10^{20}$  yr. In addition, new  $T_{1/2}$  bounds were set for different modes of  $2\beta$  processes in  $^{70}\text{Zn}$ ,  $^{180}\text{W}$ , and  $^{186}\text{W}$  at the level of  $10^{17}$ – $10^{20}$  yr.

© 2009 Elsevier B.V. All rights reserved.

PACS: 29.40.Mc; 23.40.-s

**Keywords:** RADIOACTIVITY  $^{64}\text{Zn}(2\text{EC})$ ,  $(\beta^+\text{EC})$ ;  $^{70}\text{Zn}$ ,  $^{186}\text{W}(\beta^-)$ ;  $^{180}\text{W}(2\text{EC})$ ; measured  $E_\gamma$ ,  $I_\gamma$ ; deduced  $T_{1/2}$  lower limits for various  $2\beta$ -decay modes.  $\text{ZnWO}_4$  crystal scintillator at the Gran Sasso National Laboratories

\* Corresponding author.

E-mail address: [rita.bernabei@roma2.infn.it](mailto:rita.bernabei@roma2.infn.it) (R. Bernabei).

## 1. Introduction

Neutrinoless ( $0\nu$ ) double beta ( $2\beta$ ) decay of atomic nuclei  $(A, Z) \rightarrow (A, Z \pm 2) + 2e^\mp$  is forbidden in the Standard Model (SM) because it violates the lepton number by two units [1]. However, it is predicted in many SM extensions where it is naturally expected that the neutrino is a true neutral particle equivalent to its antiparticle and has non-zero mass. While experiments on neutrino oscillations already gave evidence that the neutrino is massive [2], these experiments are sensitive only to neutrino mass differences. Double beta decay experiments are considered to-date as the best instrument to determine an absolute scale of neutrino mass, probe the nature of the neutrino (is it a Majorana particle,  $\nu = \bar{\nu}$ , or a Dirac particle,  $\nu \neq \bar{\nu}$ ?), establish the neutrino mass hierarchy, search for existence of right-handed admixtures in the weak interaction, and test some other effects beyond the SM. Developments in the experimental techniques during the last two decades lead to an impressive improvement of sensitivity to the neutrinoless mode of  $2\beta^-$  decay up to  $10^{23}$ – $10^{25}$  yr [1].

Two neutrino ( $2\nu$ ) double beta decay, a process of transformation of  $(A, Z) \rightarrow (A, Z \pm 2)$  with simultaneous emission of two electrons (or positrons) and two antineutrinos (neutrinos) is allowed in the Standard Model (SM), but being of the second order process, it is characterised by an extremely low probability: to-date it is the rarest decay observed in direct laboratory experiments. It was detected only for 10 nuclides; corresponding half-lives are in the range of  $10^{18}$ – $10^{21}$  yr [3,4].

Experimental investigations in this field are concentrated mostly on  $2\beta^-$  decays, processes featuring the emission of two electrons. Results for double positron decay ( $2\beta^+$ ), electron capture with positron emission ( $\varepsilon\beta^+$ ), and capture of two electrons from atomic shells ( $2\varepsilon$ ) are much more modest. The most sensitive experiments give limits on the  $2\varepsilon$ ,  $\varepsilon\beta^+$  and  $2\beta^+$  processes on the level of  $10^{17}$ – $10^{21}$  yr [3]. Reasons for this situation are: (1) lower energy releases in  $2\varepsilon$ ,  $\varepsilon\beta^+$  and  $2\beta^+$  processes in comparison with those in  $2\beta^-$  decay, that result in lower probabilities of the processes, as well as making background suppression difficult; (2) usually lower natural abundances of  $2\beta^+$  isotopes (which are typically lower than 1% with only few exceptions). Nevertheless, studies of neutrinoless  $2\varepsilon$  and  $\varepsilon\beta^+$  decays could help to explain the mechanism of neutrinoless  $2\beta^-$  decay (is it due to non-zero neutrino mass or to the right-handed admixtures in weak interactions) [5].

The nucleus  $^{64}\text{Zn}$  is one of the few exceptions among  $2\beta^+$  nuclei having big natural isotopic abundance (see Table 1 where properties of potentially  $2\beta$  active nuclides present in zinc tungstate ( $\text{ZnWO}_4$ ) crystals are listed). With the mass difference between  $^{64}\text{Zn}$  and  $^{64}\text{Ni}$  nuclei being 1095.7 keV [6], double electron capture and electron capture with emission of positron are energetically allowed.

Table 1  
Potentially  $2\beta$  active nuclides present in  $\text{ZnWO}_4$  crystals.

Transition	Energy release (keV) [6]	Isotopic abundance (%) [7]	Decay channels	Number of nuclei in 100 g of $\text{ZnWO}_4$ crystal
$^{64}\text{Zn} \rightarrow ^{64}\text{Ni}$	1095.7(0.7)	48.268(0.321)	$2\varepsilon, \varepsilon\beta^+$	$9.28 \times 10^{22}$
$^{70}\text{Zn} \rightarrow ^{70}\text{Ge}$	998.5(2.2)	0.631(0.009)	$2\beta^-$	$1.21 \times 10^{21}$
$^{180}\text{W} \rightarrow ^{180}\text{Hf}$	144(4)	0.12(0.01)	$2\varepsilon$	$2.31 \times 10^{20}$
$^{186}\text{W} \rightarrow ^{186}\text{Os}$	489.9(1.4)	28.43(0.19)	$2\beta^-$	$5.47 \times 10^{22}$

Table 2  
ZnWO<sub>4</sub> crystal scintillators used in the present experiments.

Crystal scintillator	Size (mm)	Mass (g)
ZWO-1	20 × 19 × 40	117
ZWO-2	∅44 × 55	699
ZWO-2a	∅44 × 14	168

It should be noted that possible evidence for  $\varepsilon\beta^+$  decay of  $^{64}\text{Zn}$ , with  $T_{1/2}^{(0\nu+2\nu)\varepsilon\beta^+} = (1.1 \pm 0.9) \times 10^{19}$  yr, was presented in Ref. [8]. Earlier experiments with CdZnTe semiconductor detectors [9] and ZnWO<sub>4</sub> crystal scintillator [10] were not sensitive enough to check this claim due to the small mass of detectors used (few grams). Experiment [11] with two detectors (HP Ge 456 cm<sup>3</sup> and CsI(Tl)  $\simeq$  400 cm<sup>3</sup>) and a 460 g Zn sample only gave a limit on the  $\varepsilon\beta^+$  decay of  $^{64}\text{Zn}$ :  $T_{1/2}^{(0\nu+2\nu)\varepsilon\beta^+} > 1.3 \times 10^{20}$  yr. Further improvements of sensitivity were reached at the first stage [12] of the experiment presented here. The measurements were performed in the Laboratori Nazionali del Gran Sasso (LNGS) of INFN (Italy) with the help of a large ZnWO<sub>4</sub> scintillator (mass of 117 g) over 1902 h. New improved half-life limits on  $2\nu$  and  $0\nu$   $\varepsilon\beta^+$  decay of  $^{64}\text{Zn}$  were established as:  $T_{1/2}^{2\nu\varepsilon\beta^+} \geq 2.1 \times 10^{20}$  yr,  $T_{1/2}^{0\nu\varepsilon\beta^+} \geq 2.2 \times 10^{20}$  yr [12]. New limits on different modes of double electron capture in  $^{64}\text{Zn}$  have been obtained too (on the level of  $10^{18}$ – $10^{19}$  yr) [12].

In addition to  $^{64}\text{Zn}$ , ZnWO<sub>4</sub> scintillators contain a few other potentially  $2\beta$  active isotopes:  $^{70}\text{Zn}$ ,  $^{180}\text{W}$  and  $^{186}\text{W}$  (see Table 1). The best to-date half-life limits on different modes and channels of  $2\beta$  processes in these isotopes were obtained in low background measurements carried out in the Solotvina Underground Laboratory with ZnWO<sub>4</sub> [10] and CdWO<sub>4</sub> [13] crystal scintillators. They are summarized later in Table 6.

Experiments [10,12] have demonstrated the good potential of ZnWO<sub>4</sub> scintillators in searching for double beta processes in Zinc and Tungsten isotopes. The main properties of ZnWO<sub>4</sub> scintillators are: (i) density equal to 7.8 g/cm<sup>3</sup>; (ii) light yield  $\simeq$  13% of that of NaI(Tl); (iii) refractive index equal to 2.1–2.2; (iv) emission maximum at 480 nm; (v) an effective average decay time of 24  $\mu$ s (at room temperature). The material is non-hygroscopic and chemically inert with melting point at 1200 °C. Radiopurity of zinc tungstate crystals has been preliminarily investigated in [10]. A development of low background ZnWO<sub>4</sub> crystal scintillators with large volume and high scintillation properties was recently realized [14].

The aim of the present work is to search for  $2\varepsilon$  capture and  $\varepsilon\beta^+$  decay of  $^{64}\text{Zn}$  with the help of large low background ZnWO<sub>4</sub> crystal scintillators. In addition, the search for double beta decays of  $^{70}\text{Zn}$ ,  $^{180}\text{W}$ , and  $^{186}\text{W}$  has been realized as a by-product of the experiment.

## 2. Experimental set-up and measurements

### 2.1. ZnWO<sub>4</sub> crystal scintillators

The ZnWO<sub>4</sub> crystal scintillators used in the present experiment (see Table 2 where the sizes and masses of the scintillators are listed) were produced from two crystal boules. The crystal boules were grown by the Czochralski method from ZnWO<sub>4</sub> compounds prepared from two batches of zinc oxide provided by different producers, and from the same tungsten oxide. The third scintillator ZWO-2a was cut from the ZWO-2 crystal.

Table 3

Contamination of ZnWO<sub>4</sub> crystal scintillators measured by ICP-MS analysis. Measured atomic masses (MAM), concentrations of elements (CE), and calculated activities of the most important radioactive isotopes (ARI) are specified.

Element (Radioactive isotope)	MAM	ZWO-1		ZWO-2	
		CE (ppb)	ARI (mBq/kg)	CE (ppb)	ARI (mBq/kg)
K ( <sup>40</sup> K)	39	≤ 15 000	≤ 500	≤ 30 000	≤ 900
Ni	60	140	–	250	–
Rb ( <sup>87</sup> Rb)	85	1.5	1.3	3.2	2.8
Cd ( <sup>113</sup> Cd)	111	670	0.001	11 000	0.02
In ( <sup>115</sup> In)	115	≤ 2.5	≤ 0.0006	≤ 5	≤ 0.0012
Sm ( <sup>147</sup> Sm)	147	≤ 4	≤ 0.5	≤ 8	≤ 1
Pt ( <sup>190</sup> Pt)	195	16	0.0002	10	0.0001
Pb	208	≤ 10	–	≤ 20	–
Th ( <sup>232</sup> Th)	232	≤ 25	≤ 100	≤ 25	≤ 100
U ( <sup>238</sup> U)	238	≤ 0.5	≤ 6	≤ 1	≤ 12

To estimate the presence of naturally occurring radioactive isotopes, as well as some other elements important for growing of the crystals, the ZnWO<sub>4</sub> samples were measured with the help of Inductively Coupled Plasma-Mass Spectrometry (ICP-MS, Agilent Technologies model 7500a).

Samples of the ZWO-1 and ZWO-2 crystals were reduced to powder by mechanical treatment inside a clean polyethylene bag to avoid contamination. The samples were etched in a microwave assisted acid digestion technique (Method EPA 3052) using nitric acid and nitric-hydrofluoric acid mixtures. The results for both procedures were just a partial sample dissolution. The solutions obtained after centrifugation have been analyzed by ICP-MS. The measurements have been carried out in semiquantitative mode. The instrumentation was calibrated with the help of a single solution containing 10 ppb of Li, Co, Y, Ce, and Tl. The concentrations of the ZnWO<sub>4</sub> samples, calculated after the procedure and after the reagents blank subtraction, are presented in Table 3. The measurements have an estimated accuracy of 20–30%. The ICP-MS detection limit for Thorium is rather low due to interference with tungsten oxide <sup>184</sup>W<sup>16</sup>O<sub>3</sub> molecule.

## 2.2. Detector, energy calibration and low background measurements

The ZnWO<sub>4</sub> crystals were fixed inside a cavity of  $\varnothing 47 \times 59$  mm in the central part of a polystyrene light-guide 66 mm in diameter and 312 mm in length. The cavity was filled up with high purity silicone oil. The light-guide was optically connected on opposite sides by optical couplant to two low radioactivity EMI9265–B53/FL 3 photomultipliers (PMT). The light-guide was wrapped by PTFE reflection tape.

The detector has been installed deep underground ( $\simeq 3600$  m w.e.) in the low background DAMA/R&D set-up at the LNGS of the INFN (Italy). It was surrounded by Cu bricks and sealed in a low radioactive air-tight Cu box continuously flushed with high purity nitrogen gas (stored deeply underground for a long time) to avoid presence of residual environmental Radon. The copper box was surrounded by a passive shield made of 10 cm of high purity Cu, 15 cm of low radioactive lead, 1.5 mm of cadmium and 4/10 cm polyethylene/paraffin to reduce the external background. The whole shield has been closed inside a Plexiglas box, also continuously flushed by high purity nitrogen gas.

Table 4

Description of low background measurements with ZnWO<sub>4</sub> crystal scintillators. Times of measurements ( $t$ ), energy intervals of data taking ( $\Delta E$ ), energy resolutions at the 662 keV  $\gamma$  line of <sup>137</sup>Cs (FWHM), and background counting rates (BG) in different energy intervals are specified.

Run	Crystal scintillator	$t$ (h)	$\Delta E$ (MeV)	FWHM (%)	BG (counts/(day×keV×kg)) in energy interval (MeV)			
					0.2–0.4	0.8–1.0	2.0–2.9	3.0–4.0
1	ZWO-1	1902	0.01–1	11.5	1.93(3)	0.27(1)		
2	ZWO-1	2906	0.05–4	12.6	1.71(2)	0.25(1)	0.0072(7)	0.0003(1)
3	ZWO-2	2130	0.05–4	14.6	1.07(1)	0.149(3)	0.0072(4)	0.00031(7)
4	ZWO-2a	3292	0.01–1	11.0	1.52(2)	0.211(7)		

An event-by-event data acquisition system accumulates the amplitude and the arrival time of the events. The sum of the signals from the PMTs was recorded with the sampling frequency of 20 MS/s over a time window of 100  $\mu$ s by a 8 bit transient digitizer (DC270 Acqiris).

The measurements were carried out in four runs (see Table 4 for details). First, the energy interval of data taking was chosen as 0.01–1 MeV with the aim to search for the neutrino accompanied double electron capture in <sup>64</sup>Zn. The data of the Run 1 has already been analyzed and published in [12]. Then the energy interval was changed to 0.05–4 MeV in order to search for other possible double beta processes in <sup>64</sup>Zn (Run 2). Then the large ZWO-2 crystal was installed and the experiment was carried out in the same energy range (Run 3). Finally the ZWO-2 crystal was cleaved in two parts; one (ZWO-2a) was used in the Run 4 with the energy interval of data taking 0.01–1 MeV.

The energy scale and resolution of the ZnWO<sub>4</sub> detectors have been measured with <sup>22</sup>Na, <sup>133</sup>Ba, <sup>137</sup>Cs, <sup>228</sup>Th and <sup>241</sup>Am  $\gamma$  sources at the beginning and end of each run. Dependence of energy resolution of the ZnWO<sub>4</sub> detectors on energy can be fitted by the function:  $\text{FWHM}_\gamma(\text{keV}) = \sqrt{a + b \cdot E_\gamma}$ , where  $E_\gamma$  is the energy of  $\gamma$  quanta in keV. For instance, the calibration energy spectra of <sup>133</sup>Ba, <sup>137</sup>Cs and <sup>241</sup>Am  $\gamma$  sources accumulated with the ZWO-2a detector are shown in Fig. 1. The values of parameters  $a$  and  $b$  for the detector are  $a = 190(40)$  keV<sup>2</sup> and  $b = 7.34(35)$  keV. The energy resolutions of the ZnWO<sub>4</sub> detectors for 662 keV  $\gamma$  quanta of <sup>137</sup>Cs are presented in Table 4. In addition, the energy scale of the detectors was checked by using background  $\gamma$  lines of 609 keV of <sup>214</sup>Bi (in all Runs), 1461 keV (<sup>40</sup>K), 1764 keV (<sup>214</sup>Bi), 2615 keV (<sup>208</sup>Tl) in Runs 2 and 3. The energy scales during all four Runs were reasonably stable with deviations in the range of 2–3%.

The relative light yield for  $\alpha$  particles as compared with that for  $\gamma$  quanta ( $\beta$  particles) — the so-called  $\alpha/\beta$  ratio<sup>1</sup> — was derived from the measurements [10]:  $\alpha/\beta = 0.074(16) + 0.0164(40) \times E_\alpha$ , where  $E_\alpha$  is the energy of  $\alpha$  particles in MeV ( $E_\alpha > 2$  MeV).

The energy spectra accumulated over Runs 2 and 3 with the ZnWO<sub>4</sub> detectors in the low background set-up are shown in Fig. 2. The spectra are normalized to the mass of the crystals and time of the measurements. A few peaks in the spectra can be ascribed to  $\gamma$  quanta of naturally occurring radionuclides <sup>40</sup>K, <sup>214</sup>Bi (<sup>238</sup>U chain) and <sup>208</sup>Tl (<sup>232</sup>Th) from the materials of the set-up. The background counting rates of the ZnWO<sub>4</sub> detectors for Runs 1–4 in the energy intervals 0.2–0.4, 0.8–1.0, 2.0–2.9, and 3.0–4.0 MeV are given in Table 4.

<sup>1</sup> The  $\alpha/\beta$  ratio is defined as the ratio of  $\alpha$  peak position in the energy scale measured with  $\gamma$  sources to the energy of  $\alpha$  particles ( $E_\alpha$ ). Because  $\gamma$  quanta interact with the detector by  $\beta$  particles, we use more convenient term “ $\alpha/\beta$ ” ratio.

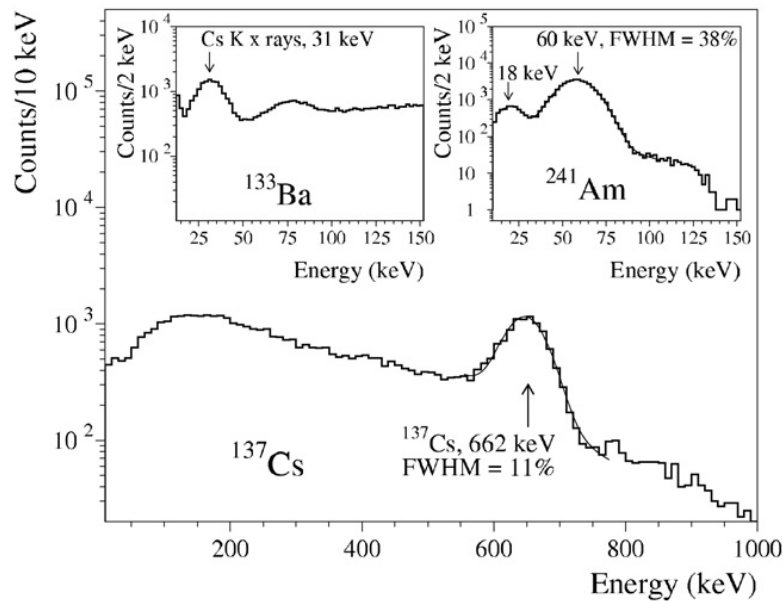


Fig. 1. Energy spectra measured by  $\text{ZnWO}_4$  detector (ZWO-2a) with  $^{137}\text{Cs}$  (main part),  $^{133}\text{Ba}$  and  $^{241}\text{Am}$  (inserts)  $\gamma$  sources.

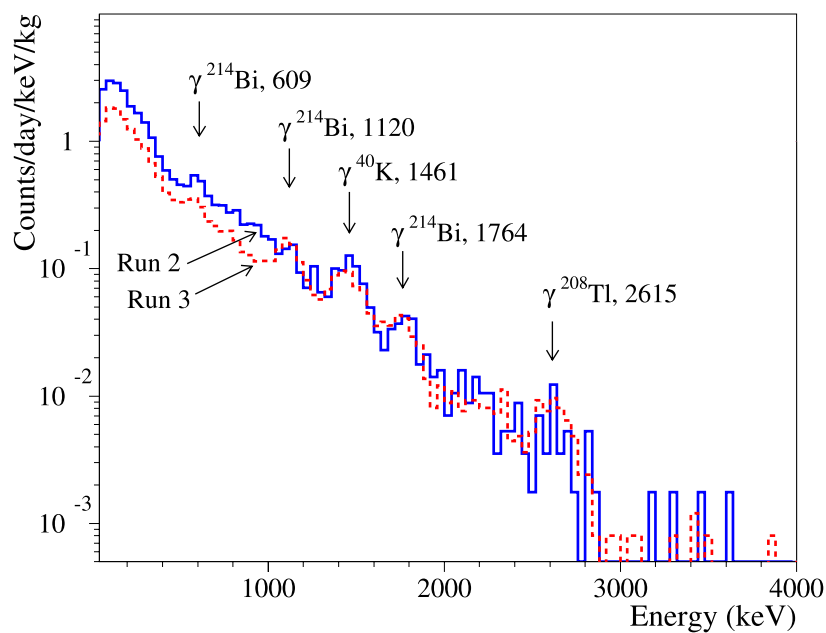


Fig. 2. (Color online.) Energy spectra of  $\text{ZnWO}_4$  scintillators measured in the low background set-up during Run 2 (solid line) and Run 3 (dashed line). Energies of  $\gamma$  lines are in keV.

### 3. Data analysis

Knowledge of the radioactive contamination of the  $\text{ZnWO}_4$  crystals is necessary to describe the measured background spectra. The time-amplitude analysis, the pulse-shape discrimination, and the Monte Carlo simulation were applied to reconstruct the background spectra and to estimate the radioactive contamination of the  $\text{ZnWO}_4$  detectors.

### 3.1. Time-amplitude analysis

The arrival time and energy of each event were used for the selection of the following fast decay chain in the  $^{232}\text{Th}$  family<sup>2</sup>:  $^{220}\text{Rn}$  ( $Q_\alpha = 6.41$  MeV,  $T_{1/2} = 55.6$  s)  $\rightarrow$   $^{216}\text{Po}$  ( $Q_\alpha = 6.91$  MeV,  $T_{1/2} = 0.145$  s)  $\rightarrow$   $^{212}\text{Pb}$ . All events within 0.75–1.75 MeV were used as triggers, while a time interval 0.025–0.3 s (65% of  $^{216}\text{Po}$  decays) and the same energy window were set for the second events. Four and seven events of the fast chain  $^{224}\text{Ra} \rightarrow ^{220}\text{Rn} \rightarrow ^{216}\text{Po} \rightarrow ^{212}\text{Pb}$  were found in the data of Run 2 and Run 3, respectively. Taking into account the efficiency of the events selection in the time interval, one can calculate the activities of  $^{228}\text{Th}$  in the  $\text{ZnWO}_4$  crystals as 5(3)  $\mu\text{Bq/kg}$  (ZWO-1), and 2(1)  $\mu\text{Bq/kg}$  (ZWO-2).

Similarly the limits on activity of  $^{227}\text{Ac}$  ( $^{235}\text{U}$  family) in the crystals were set by selection of the fast chain  $^{219}\text{Rn}$  ( $Q_\alpha = 6.95$  MeV,  $T_{1/2} = 3.96$  s)  $\rightarrow$   $^{215}\text{Po}$  ( $Q_\alpha = 7.53$  MeV,  $T_{1/2} = 1.78$  ms)  $\rightarrow$   $^{211}\text{Pb}$ . The activity of  $^{227}\text{Ac}$  was restricted to  $\leq 7$   $\mu\text{Bq/kg}$  in the ZWO-1 and  $\leq 3$   $\mu\text{Bq/kg}$  in the ZWO-2 crystal.

### 3.2. Pulse-shape discrimination between $\beta(\gamma)$ and $\alpha$ particles

As demonstrated in [10], the difference in pulse shapes in the  $\text{ZnWO}_4$  scintillator allows one to discriminate  $\gamma(\beta)$  events from those induced by  $\alpha$  particles. The optimal filter method proposed by E. Gatti and F. De Martini in 1962 [17] was applied for this purpose. For each signal  $f(t)$ , the numerical characteristic of its shape (shape indicator,  $SI$ ) was defined as  $SI = \sum f(t_k) \times P(t_k) / \sum f(t_k)$ , where the sum is over the time channels  $k$ , starting from the origin of signal and averaging up to 50  $\mu\text{s}$ ;  $f(t_k)$  is the digitized amplitude (at the time  $t_k$ ) of a given signal. The weight function  $P(t)$  was defined as:  $P(t) = \{f_\alpha(t) - f_\gamma(t)\} / \{f_\alpha(t) + f_\gamma(t)\}$ , where  $f_\alpha(t)$  and  $f_\gamma(t)$  are the reference pulse shapes for  $\alpha$  particles and  $\gamma$  quanta, respectively, obtained by summing up shapes of a few thousand  $\gamma$  or  $\alpha$  events. The scatter plot of the shape indicator versus energy for the data of the low background measurements in Run 3 is depicted in Fig. 3. The distribution of shape indicators for the events with the energies in the energy interval 0.5–1.0 MeV is depicted in the Inset of Fig. 3. They are well described by Gaussian functions. The population of  $\alpha$  events is clearly separated from  $\gamma(\beta)$  events.

The energy spectra of  $\gamma(\beta)$  and  $\alpha$  events selected with the help of the pulse-shape discrimination from data of Run 3 are shown in Fig. 4. As was demonstrated in [10], the energy resolution for  $\alpha$  particles is considerably worse than that for  $\gamma$  quanta due to dependence of the  $\alpha/\beta$  ratio on the direction of  $\alpha$  particles relative to the  $\text{ZnWO}_4$  crystal axes. It hampers discrimination between alpha peaks of U/Th  $\alpha$  active daughters. Therefore, we can only set limits on activities of the nuclides in the  $\text{ZnWO}_4$  crystals. The total activities of  $\alpha$  active U/Th daughters are 0.38(5) mBq/kg and 0.18(3) mBq/kg in the ZWO-1 and ZWO-2 crystals, respectively. There are no peculiarities in the low energy region of the  $\alpha$  spectrum where an  $\alpha$  peak of  $^{147}\text{Sm}$  could be present. The fit of the spectra in the energy interval 140 – 470 keV by a simple model, based on a first degree polynomial function (to describe the background) and a Gaussian function ( $\alpha$  peak of  $^{147}\text{Sm}$ ), only gives a limit on  $^{147}\text{Sm}$  activity in the ZWO-1 and ZWO-2 crystal scintillators:  $\leq 0.01$  mBq/kg.

Search for the fast decays  $^{214}\text{Bi}$  ( $Q_\beta = 3.27$  MeV,  $T_{1/2} = 19.9$  m)  $\rightarrow$   $^{214}\text{Po}$  ( $Q_\alpha = 7.83$  MeV,  $T_{1/2} = 164$   $\mu\text{s}$ )  $\rightarrow$   $^{210}\text{Pb}$  (in equilibrium with  $^{226}\text{Ra}$  from the  $^{238}\text{U}$  chain) was performed with

<sup>2</sup> The technique of the time-amplitude analysis is described in detail in [15,16].



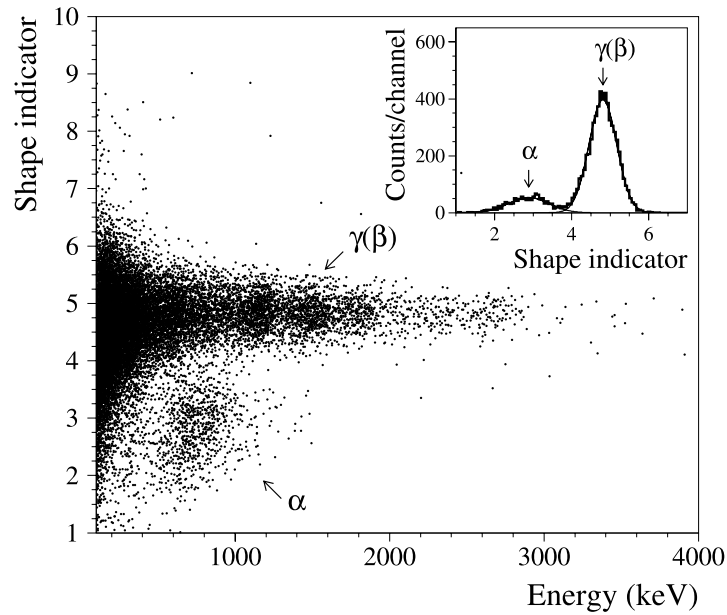


Fig. 3. Scatter plot of the shape indicator (see text) versus energy for 2130 h background exposition with the ZWO-2 crystal scintillator. (Inset) Distribution of shape indicators for the data selected in the energy interval 0.5–1.0 MeV. Fit of the distribution by two Gaussian functions is shown by solid lines.

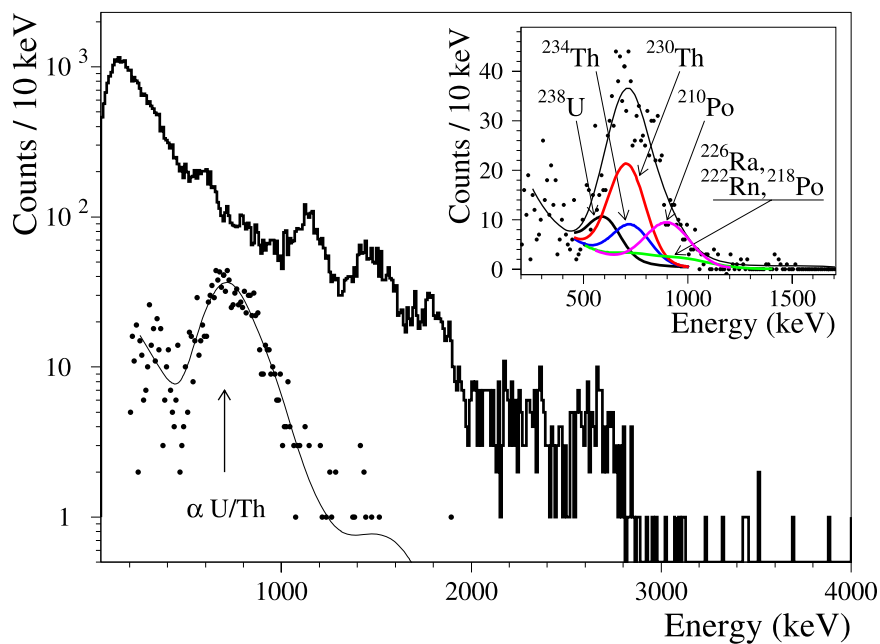


Fig. 4. (Color online.) The energy spectrum of  $\beta$  particles ( $\gamma$  quanta, solid histogram) and  $\alpha$  particles (dots) selected by the pulse-shape discrimination from raw data measured with the ZWO-2 scintillator during 2130 h in the low background set-up. In the inset, the  $\alpha$  spectrum is depicted together with the model, which includes  $\alpha$  decays from  $^{238}\text{U}$  family.

the help of pulse-shape analysis of double pulses.<sup>3</sup> The activity of  $^{226}\text{Ra}$  in the ZWO-2 crystal was estimated as 0.002(1) mBq/kg, and a limit of  $\leq 0.01$  mBq/kg for Radium contamination in the ZWO-1 detector was provided by the analysis.

<sup>3</sup> The technique of the analysis is described in [13,18].

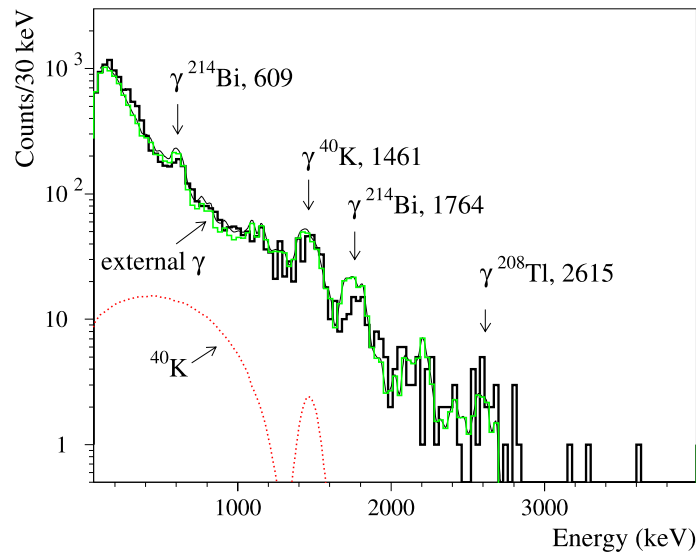


Fig. 5. (Color online.) Energy spectrum of  $\beta(\gamma)$  events accumulated in the low background set-up with the ZWO-1 crystal scintillator over 2906 h (Run 2) together with the model of the background. The main components of the background are shown: spectrum of  $^{40}\text{K}$  (internal contamination), and the contribution from the external  $\gamma$  quanta from PMTs in these experimental conditions.

### 3.3. Simulation of $\beta(\gamma)$ background

There are several  $\beta$  active radionuclides ( $^{40}\text{K}$ ,  $^{60}\text{Co}$ ,  $^{87}\text{Rb}$ ,  $^{90}\text{Sr}$ – $^{90}\text{Y}$ ,  $^{137}\text{Cs}$ , some U/Th daughters such as  $^{234m}\text{Pa}$ ,  $^{214}\text{Pb}$ ,  $^{214}\text{Bi}$ ,  $^{210}\text{Pb}$ ,  $^{210}\text{Bi}$ ,  $^{228}\text{Ac}$ ,  $^{212}\text{Bi}$ ,  $^{208}\text{Th}$ ) which could produce background in the  $\text{ZnWO}_4$  detectors. Radioactive contamination of the PMTs could also contribute to the background. The energy distributions of the possible background components were simulated with the help of the GEANT4 package [19]. The initial kinematics of the particles emitted in the decay of nuclei was given by an event generator DECAY0 [20].

The measured background spectra were fitted by the model built from the simulated distributions. Activities of U/Th daughters in the crystals were restricted taking into account the results of the time-amplitude and pulse-shape analyzes. Activities of  $\beta$  active  $^{87}\text{Rb}$ ,  $^{113}\text{Cd}$ , and  $^{115}\text{In}$  were bounded taking into account the results of the ICP-MS analysis. The initial values of the  $^{40}\text{K}$ ,  $^{232}\text{Th}$  and  $^{238}\text{U}$  activities inside the PMTs were taken from [21] where the radioactive contamination of PMTs of the same model were measured. The peak in the spectrum of Run 3 at the energy  $1133 \pm 8$  keV cannot be explained by a contribution from external  $\gamma$  rays (the 1120 keV  $\gamma$  line of  $^{214}\text{Bi}$  is not intense enough to provide the whole peak area). We assume the presence of  $^{65}\text{Zn}$  ( $T_{1/2} = 244.26$  d,  $Q_{\beta} = 1351.9$  keV [22]) in the crystal to explain the peak.  $^{65}\text{Zn}$  can be produced from  $^{64}\text{Zn}$  by thermal neutrons (the cross section of  $^{64}\text{Zn}$  to thermal neutrons is 0.76 barn [22]) or/and by cosmogenic activation. The fit of the spectrum of Run 3 gives an activity of 0.5 mBq/kg in the ZWO-2 crystal, and only a limit of  $\leq 0.8$  mBq/kg in the ZWO-1 crystal. There are no other clear peculiarities in the spectra which could be ascribed to the internal trace contamination by radioactive nuclides. Therefore we can only obtain limits on the activities of the  $\beta$  active radionuclides and U/Th daughters. The result of the fit of the spectra of Run 2 and Run 3 in the energy region 0.1–2.9 MeV and the main components of the background are shown in Figs. 5 and 6. The summary of radioactive contamination of the  $\text{ZnWO}_4$  crystal scintillators (or limits on their activities) is given in Table 5.

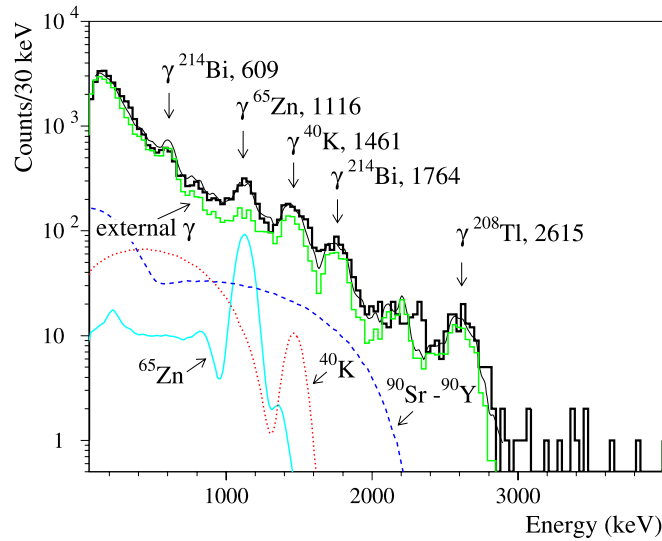


Fig. 6. (Color online.) Energy spectrum of  $\beta(\gamma)$  events accumulated in the low background set-up with the ZWO-2 crystal scintillator over 2130 h (Run 3) together with the model of the background. The main components of the background are shown: spectra of  $^{40}\text{K}$ ,  $^{90}\text{Sr}$ - $^{90}\text{Y}$ ,  $^{65}\text{Zn}$ , and the contribution from the external  $\gamma$  quanta from PMTs in these experimental conditions.

Table 5  
Radioactive contamination of  $\text{ZnWO}_4$  scintillators determined by different methods.

Chain	Nuclide	Activity (mBq/kg)	
		ZWO-1	ZWO-2
$^{232}\text{Th}$	$^{232}\text{Th}$	$\leq 0.11^a$	$\leq 0.1^a$
	$^{228}\text{Ra}$	$\leq 0.2^b$	$\leq 0.05^b$
	$^{228}\text{Th}$	$0.005(3)^c$	$0.002(1)^c$
$^{235}\text{U}$	$^{227}\text{Ac}$	$\leq 0.007^c$	$\leq 0.003^c$
$^{238}\text{U}$	$^{238}\text{U}$	$\leq 0.1^a$	$\leq 0.08^a$
	$^{230}\text{Th}$	$\leq 0.13^a$	$\leq 0.07^a$
	$^{226}\text{Ra}$	$\leq 0.006^a$	$0.002(1)^a$
	$^{210}\text{Po}$	$\leq 0.2^a$	$\leq 0.06^a$
Total $\alpha$ activity		$0.38(5)^a$	$0.18(3)^a$
	$^{40}\text{K}$	$\leq 1^b$	$\leq 0.4^b$
	$^{60}\text{Co}$	$\leq 0.05^b$	$\leq 0.1^b$
	$^{65}\text{Zn}$	$\leq 0.8^b$	$0.5^b$
	$^{87}\text{Rb}$	$1.3^d, \leq 2.6^b$	$2.8^d, \leq 2.3^b$
	$^{90}\text{Sr}$ - $^{90}\text{Y}$	$\leq 0.6^b$	$\leq 0.4^b$
	$^{137}\text{Cs}$	$\leq 0.3^b$	$\leq 0.05^b$
	$^{147}\text{Sm}$	$\leq 0.01^a$	$\leq 0.01^a$

<sup>a</sup> Pulse-shape discrimination (see Section 3.2).

<sup>b</sup> Fit of background spectra (see Section 3.3).

<sup>c</sup> Time-amplitude analysis (see Section 3.1).

<sup>d</sup> ICP-MS analysis (see Section 2.1).

#### 4. Results and discussion

There are no clear peculiarities in the measured energy spectra of the  $\text{ZnWO}_4$  detectors, which can be interpreted as double beta decay of Zinc or Tungsten isotopes. Therefore only lower half-life limits can be set according to the formula:

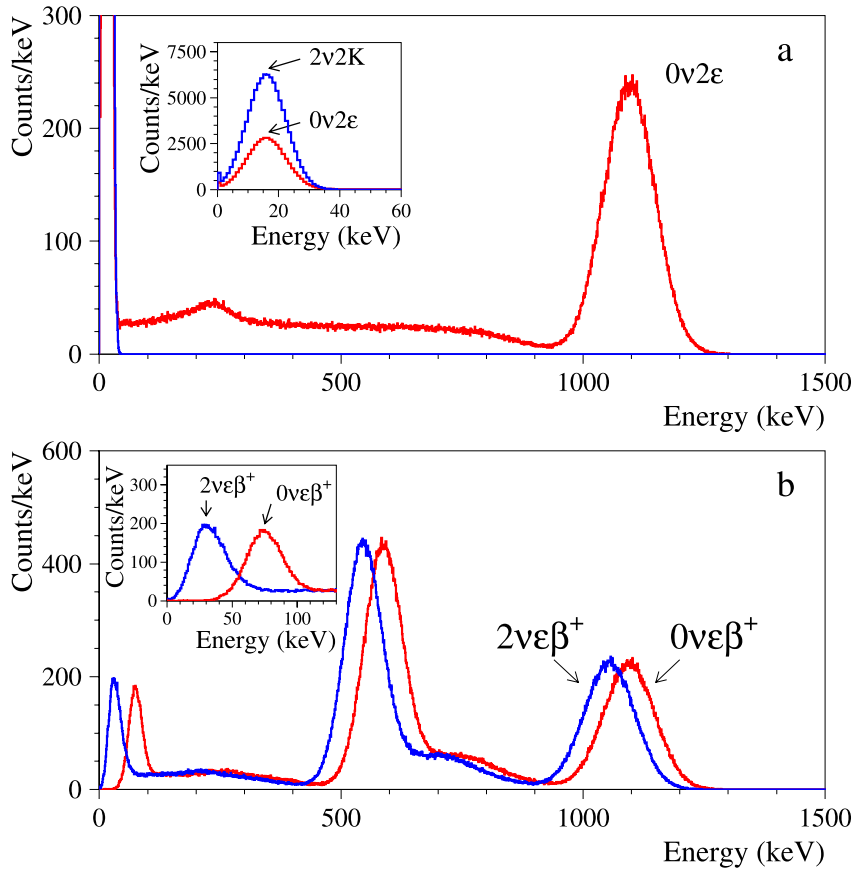


Fig. 7. (Color online.) Simulated response functions of the ZWO-2 scintillator for two neutrino and neutrinoless  $2\varepsilon$  (a) and  $\varepsilon\beta^+$  (b) decays in  $^{64}\text{Zn}$ . One million of decays was simulated for each mode.

$$\lim T_{1/2} = N \cdot \eta \cdot t \cdot \ln 2 / \lim S,$$

where  $N$  is the number of potentially  $2\beta$  unstable nuclei,  $\eta$  is the detection efficiency,  $t$  is the measuring time, and  $\lim S$  is the number of events of the effect searched for which can be excluded at a given confidence level (C.L.).

We have used different combinations of the accumulated data to reach maximal sensitivity to the sought double beta processes. The response functions of the  $\text{ZnWO}_4$  detectors for the  $2\beta$  processes were simulated with the help of the GEANT4 code [19]. The initial kinematics of the particles emitted in the decays was generated with the DECAY0 event generator [20].

#### 4.1. Search for double electron capture and $\varepsilon\beta^+$ decay of $^{64}\text{Zn}$

The energy distributions for the  $2\beta$  processes in  $^{64}\text{Zn}$  expected for the ZWO-2 detector are shown in Fig. 7. It should be stressed that the detection efficiencies in the whole distributions are at least 99.9% for all the processes.

Two approaches were used to estimate the value of  $\lim S$  for the mode of the two neutrino electron capture with positron emission ( $2\nu\varepsilon\beta^+$ ) in  $^{64}\text{Zn}$ . In the first one (the so-called  $1\sigma$  approach) statistical uncertainty of the number of events registered in the energy region of the expected peak was taken as  $\lim S$ . There were 11,848 events observed in the energy interval 490–1150 keV of the spectrum (Run 2 + Run 3, see Fig. 8), which gives  $\lim S = 109$  counts. Considering the related efficiency in the energy interval (82%), it gives the half-life limit  $T_{1/2}^{2\nu\varepsilon\beta^+} \geq 1.0 \times 10^{21}$  yr.

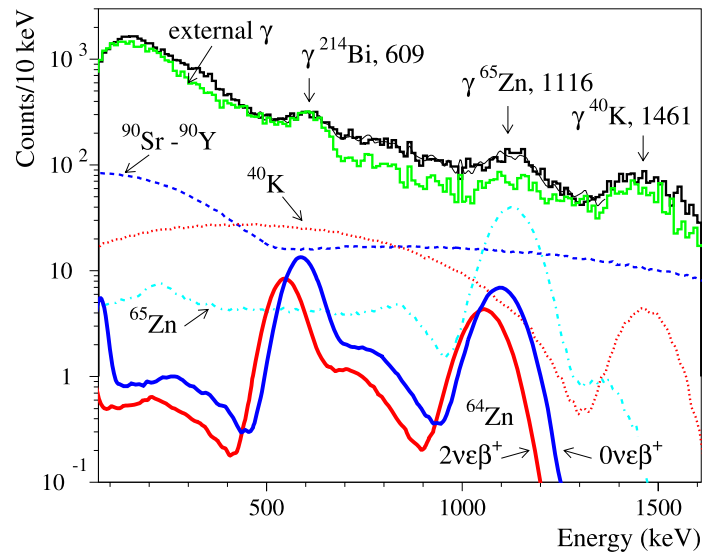


Fig. 8. (Color online.) The measured energy spectrum of  $\text{ZnWO}_4$  scintillation crystals (Run 2 + Run 3) together with the response functions for  $\varepsilon\beta^+$  process in  $^{64}\text{Zn}$  excluded at 90% C.L. Most important components of the background are shown. The energies of  $\gamma$  lines are in keV.

In the second approach the energy spectrum was fitted in the energy range 380–1430 keV by model functions. The background model was composed of  $^{40}\text{K}$ ,  $^{60}\text{Co}$ ,  $^{65}\text{Zn}$ ,  $^{90}\text{Sr}$ – $^{90}\text{Y}$ ,  $^{137}\text{Cs}$ , U/Th inside crystal, and  $^{40}\text{K}$ ,  $^{232}\text{Th}$ ,  $^{238}\text{U}$  in the PMTs. The starting and final energies of the fit were varied as 380–460 keV and 1260–1430 keV, respectively, with a step of 10 keV. The result of the fit in the energy region 430–1360 keV was chosen so as to give the minimal value of  $\chi^2/n.d.f. = 121/80 = 1.51$ . It gives the total area of the  $2\nu\varepsilon\beta^+$  effect as  $-232 \pm 235$  counts which corresponds (in accordance with the Feldman–Cousins procedure [23]) to  $\text{lim } S = 192(65)$  counts at 90% (68%) C.L. One can calculate the following half-life limit (here and hereafter all the half-life limits and values of  $\text{lim } S$  are presented at 90% (68%) C.L.):

$$T_{1/2}^{2\nu\varepsilon\beta^+} (^{64}\text{Zn}) \geq 0.70(2.1) \times 10^{21} \text{ yr.}$$

The situation with the neutrinoless  $2\varepsilon$  and  $\varepsilon\beta^+$  processes is more complicated due to the presence of the  $1133 \pm 8$  keV peak in the background spectra of Run 3. One could suppose that this peak is due to the  $0\nu 2\varepsilon$  or/and  $0\nu\varepsilon\beta^+$  decay of  $^{64}\text{Zn}$ . However, there are several arguments against such an assumption:

- (1) the energy of the higher energy peak in the simulated distribution of  $0\nu\varepsilon\beta^+$  and  $0\nu 2\varepsilon$  decay of  $^{64}\text{Zn}$  is 1096 keV (see Fig. 7), while the energy of the peak in the spectrum of  $^{65}\text{Zn}$  is 1125 keV, which is a better candidate for explaining the observed peak;
- (2) there is no such peak in the spectrum of Run 2;
- (3) a fit of the spectrum Run 2 + Run 3 in the energy interval 440–1350 keV by the model without the  $^{65}\text{Zn}$  distribution is much worse ( $\chi^2/n.d.f. = 179/78 = 2.29$ ), than that with the distribution of  $^{65}\text{Zn}$  added to the model of the background.

In the last case the fit of the spectrum in the same energy interval gives essentially a smaller value of  $\chi^2/n.d.f. = 112/77 = 1.45$ . The fit gives the area of the effect searched for as  $116 \pm$

119, which corresponds to  $\lim S = 311(235)$  events. It sets the following limit on the half-life of  $^{64}\text{Zn}$  relative to the  $0\nu\varepsilon\beta^+$  decay:

$$T_{1/2}^{0\nu\varepsilon\beta^+} (^{64}\text{Zn}) \geq 4.3(5.7) \times 10^{20} \text{ yr.}$$

Theoretical calculations of probability of neutrinoless electron capture with positron emission in  $^{64}\text{Zn}$  are absent in the literature. To estimate a value of the effective neutrino mass which corresponds to the obtained half-life, we can assume (very optimistically) a theoretical value of the product of half-life with the effective neutrino mass as<sup>4</sup>  $T_{1/2} \cdot m_\nu^2 = 10^{26} - 10^{29} \text{ yr eV}^2$ . It gives the value of the effective neutrino mass  $m_\nu \sim 1 - 10 \text{ keV}$ . It is clear that ascribing the observed at 1.1 MeV peak to  $0\nu\varepsilon\beta^+$  decay of  $^{64}\text{Zn}$  (instead of ascribing it to background from  $^{65}\text{Zn}$ ) would be in strong contradiction with the results of the most sensitive  $2\beta^-$  decay experiments which give limits on the neutrino mass on the level of  $\sim 1 \text{ eV}$  [1].

The energy distributions expected for the  $2\nu\varepsilon\beta^+$  and  $0\nu\varepsilon\beta^+$  decay of  $^{64}\text{Zn}$ , excluded at 90% C.L., are shown in Fig. 8.

In case of  $0\nu 2\varepsilon$  decay, different particles are emitted: X-rays and Auger electrons from de-excitations in atomic shells, and  $\gamma$  quanta and/or conversion electrons from de-excitation of a daughter nucleus. We suppose here that in the nuclear de-excitation process only one  $\gamma$  quantum is emitted that is the most pessimistic scenario from the point of view of registration of such an event in a peak of full absorption at the  $Q_{2\beta}$  energy.  $2K$ ,  $KL$ ,  $2L$  (and other) modes are not energetically resolved in the high energy region because of the finite energy resolution of the detector (see Fig. 7a). A fit of the measured spectrum in the energy interval 430–1300 keV gives the following limit:

$$T_{1/2}^{0\nu 2\varepsilon} (^{64}\text{Zn}) \geq 1.1(2.8) \times 10^{20} \text{ yr.}$$

#### 4.2. Search for $2\beta^-$ decay of $^{186}\text{W}$ and $^{70}\text{Zn}$

The expected energy spectra for different channels of  $2\beta$  decay of  $^{186}\text{W}$  are shown in the Inset of Fig. 9.

The energy spectrum (Run 1 + Run 2 + Run 3 + Run 4) was used to search for  $2\beta^-$  decays of  $^{186}\text{W}$  to the ground state and to the first excited ( $2_1^+$ ) level of  $^{186}\text{Os}$  ( $E_{\text{exc}} = 137 \text{ keV}$ ). The “One sigma” approach gives the same limit of  $T_{1/2}^{0\nu 2\beta} \geq 1.1 \times 10^{21} \text{ yr}$  for both transitions (because of practically the same detection efficiencies:  $\eta = 99.2\%$  and  $\eta = 97.6\%$  in the energy interval 400–600 keV for transitions to the ground and to the excited states, respectively). A fit in the energy interval 380–620 keV gives the limit:

$$T_{1/2}^{0\nu 2\beta} (^{186}\text{W}, \text{ g.s. and } 2_1^+) \geq 2.1(4.2) \times 10^{20} \text{ yr.}$$

Fitting the spectra accumulated in Run 3 in the energy interval 190–450 keV allows to set the limit on the  $0\nu 2\beta$  decay with Majoron emission:

$$T_{1/2}^{0\nu 2\beta M1} (^{186}\text{W}, \text{ g.s.}) \geq 5.8(8.6) \times 10^{19} \text{ yr.}$$

<sup>4</sup> Such a level of half-life for  $0\nu\varepsilon\beta^+$  process was obtained in theoretical calculations for  $^{96}\text{Ru}$ , one of the most promising  $2\beta^+$  nuclei [5,24,25].

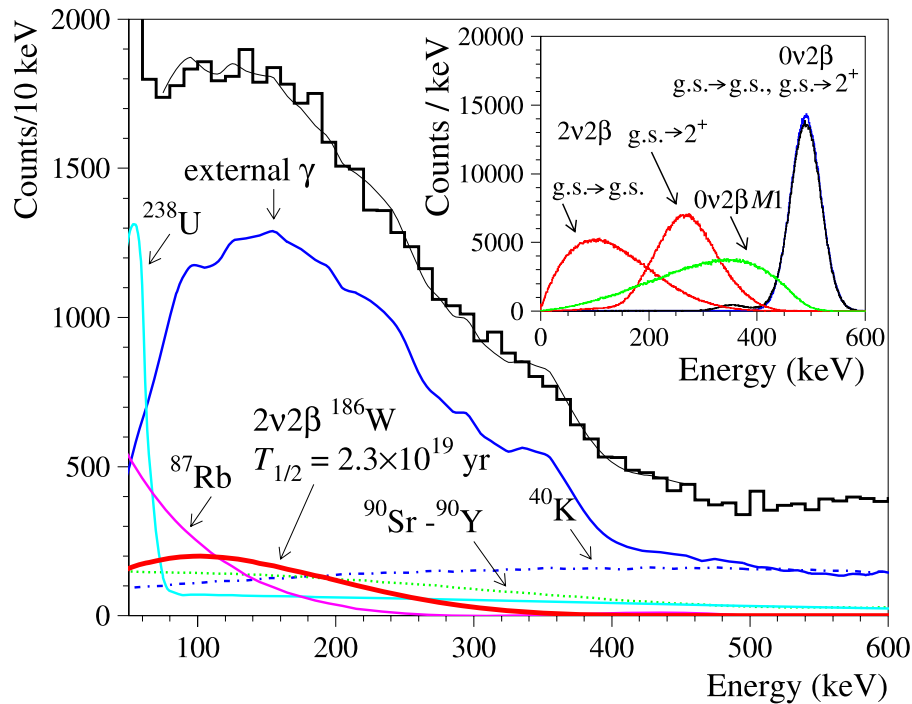


Fig. 9. (Color online.) Energy spectrum of background obtained by sum of Runs 3 and 4 together with fit and main components of the background (external  $\gamma$  rays from PMT, internal  $^{40}\text{K}$ ,  $^{87}\text{Rb}$ ,  $^{90}\text{Y}$ - $^{90}\text{Sr}$ ,  $^{238}\text{U}$ ). The simulated response function for  $2\nu 2\beta$  decay of  $^{186}\text{W}$  with the half-life  $T_{1/2}^{2\nu 2\beta} = 2.3 \times 10^{19}$  yr excluded at 68% is also shown. (Inset) Simulated response functions for different double beta processes in  $^{186}\text{W}$ . The distribution for  $0\nu 2\beta$  decay to the ground state of  $^{186}\text{Os}$  is practically indistinguishable from the peak of  $0\nu 2\beta$  decay to the  $2^+$  excited state of  $^{186}\text{Os}$ .

The best sensitivity to the two neutrino mode of  $2\beta$  decay of  $^{186}\text{W}$  was achieved by analysis of the spectrum of Run 3 + 4 (see Fig. 9). Fit in the energy interval 70–450 keV gives the number of events  $2037 \pm 1125$  which corresponds to  $\text{lim } S = 3882(3162)$ . It sets the half-life limit:

$$T_{1/2}^{2\nu 2\beta} (^{186}\text{W}, \text{g.s.}) \geq 2.3(2.8) \times 10^{19} \text{ yr.}$$

Fit of the spectrum (Run 1 + Run 2 + Run 3 + Run 4) in the energy interval 190–450 keV gives the following restriction for the half-life relative to the  $2\nu 2\beta$  decay of  $^{186}\text{W}$  to the first excited level  $2_1^+$  of  $^{186}\text{Os}$ :

$$T_{1/2}^{2\nu 2\beta} (^{186}\text{W}, 2_1^+) \geq 1.8(3.6) \times 10^{20} \text{ yr.}$$

Similarly, the limits on  $2\beta^-$  processes in  $^{70}\text{Zn}$  were obtained. The sum of energy spectra measured in Runs 2 and 3 was used to search for  $0\nu 2\beta$  decay of  $^{70}\text{Zn}$ , while the sum of all the accumulated spectra was taken to set limits on the two neutrino mode of double beta decay and the  $0\nu 2\beta$  decay with Majoron emission.

It should be noted that in accordance with theoretical calculations in the pseudo SU(3) framework [26] which take into account deformation of the  $^{186}\text{W}$  nucleus (in contrast with the standard QRPA method), the  $2\nu 2\beta$  decay rate of  $^{186}\text{W}$  could be strongly suppressed, or even vanishingly small. Hence, the energy region of  $0\nu 2\beta$  signal of  $^{186}\text{W}$  would be free from the background created by the  $2\nu 2\beta$  events, which can reach this region due to the poor energy resolution of the detector. The suppression of the  $2\nu$  mode would be especially important in the search for the  $0\nu$  decay with Majoron emission, whose distribution is continuous, because in this case the

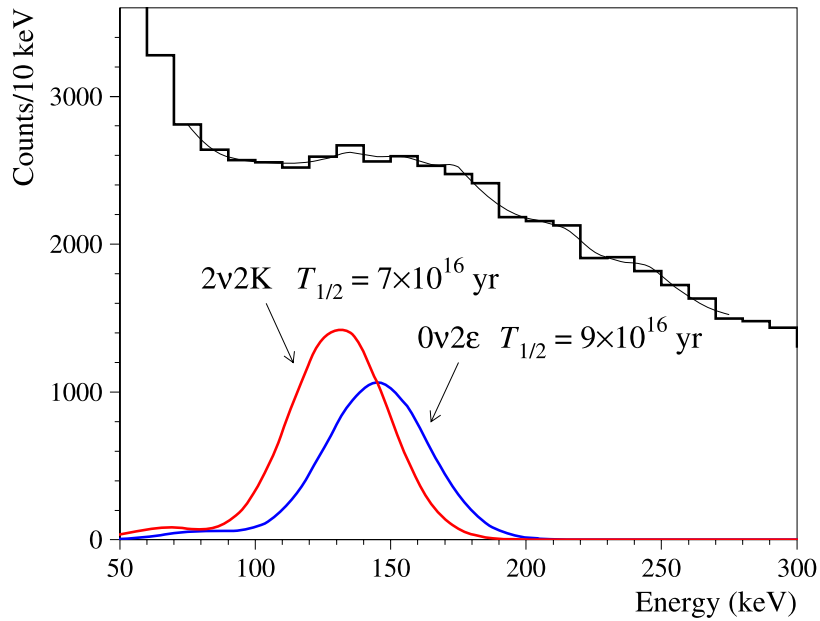


Fig. 10. (Color online.) Energy spectrum of background obtained by sum of all Runs together with fit in the energy interval 70–270 keV. The simulated response functions for double electron capture in  $^{180}\text{W}$  are shown; the half-lives  $T_{1/2}^{2\nu 2K} = 7 \times 10^{16}$  yr and  $T_{1/2}^{0\nu 2\varepsilon} = 9 \times 10^{16}$  yr correspond to the best previous limits reported in [13].

$0\nu 2\beta M1$  events will not be distinguished from the  $2\nu$  background even with the help of the high energy resolution detector.

#### 4.3. $2\varepsilon$ capture in $^{180}\text{W}$

The sum of the background spectra of the  $\text{ZnWO}_4$  detectors accumulated in all four Runs was used to set limits on the  $0\nu 2\varepsilon$  process in  $^{180}\text{W}$ . The low energy part of the spectrum is shown in Fig. 10. The least squares fit of this spectrum in the 70–270 keV energy interval gives  $133 \pm 256$  counts for the  $0\nu 2\varepsilon$  peak searched for ( $\chi^2/n.d.f. = 12.8/7 = 1.83$ ), providing no evidence for the effect. These numbers lead to an upper limit of 553(389) counts. Taking into account detection efficiency for this process close to 1, one can calculate the half-life limit:

$$T_{1/2}^{0\nu 2\varepsilon} (^{180}\text{W}) \geq 0.86(1.2) \times 10^{18} \text{ yr.}$$

The same method gives the restriction for the  $2\nu 2K$  process in  $^{180}\text{W}$ :

$$T_{1/2}^{2\nu 2K} (^{180}\text{W}) \geq 6.6(9.4) \times 10^{17} \text{ yr.}$$

The response functions for  $0\nu 2\varepsilon$  and  $2\nu 2K$  decay of  $^{180}\text{W}$  corresponding to the best previous limits obtained in [13] are presented in Fig. 10.

All the half-life limits on  $2\beta$  decay processes in Zinc and Tungsten obtained in the present experiment are summarized in Table 6 where results of the most sensitive previous experiments are given for comparison.

The obtained bounds are well below the existing theoretical predictions [27,28]; nevertheless most of the limits are near one order of magnitude higher than those established in previous experiments. It should be stressed that in contrast to a level of sensitivity obtained for double  $\beta^-$  decay ( $10^{23}$ – $10^{25}$  years in the best experiments), only two nuclei ( $^{40}\text{Ca}$  and  $^{78}\text{Kr}$ ) among potentially  $2\varepsilon$ ,  $\varepsilon\beta^+$ ,  $2\beta^+$  active isotopes were investigated at the level of  $\sim 10^{21}$  yr.



Table 6  
Half-life limits on  $2\beta$  processes in Zn and W isotopes.

Transition	Decay channel	Level of daughter nucleus	$T_{1/2}$ limit (yr)	
			Present work 90% (68%) C.L.	Previous results 90% (68%) C.L.
$^{64}\text{Zn} \rightarrow ^{64}\text{Ni}$	$0\nu 2\varepsilon$	g.s.	$\geq 1.1(2.8) \times 10^{20}$	$\geq 0.7(1.0) \times 10^{18}$ [10] $\geq 3.4(5.5) \times 10^{18}$ [12]
	$0\nu\varepsilon\beta^+$	g.s.	$\geq 4.3(5.7) \times 10^{20}$	$\geq 2.8 \times 10^{16}$ [9] $\geq 2.4(3.6) \times 10^{18}$ [10] $\geq 1.3 \times 10^{20}$ [11] $\geq 2.2(6.1) \times 10^{20}$ [12]
	$2\nu\varepsilon\beta^+$	g.s.	$\geq 0.70(2.1) \times 10^{21}$	$= (1.1 \pm 0.9) \times 10^{19}$ [8] $\geq 4.3(8.9) \times 10^{18}$ [10] $\geq 1.3 \times 10^{20}$ [11] $\geq 2.1(7.4) \times 10^{20}$ [12]
$^{70}\text{Zn} \rightarrow ^{70}\text{Ge}$	$0\nu 2\beta^-$	g.s.	$\geq 1.8(3.0) \times 10^{19}$	$\geq 0.7(1.4) \times 10^{18}$ [10]
	$2\nu 2\beta^-$	g.s.	$\geq 2.3(4.0) \times 10^{17}$	$\geq 1.3(2.1) \times 10^{16}$ [10]
	$0\nu 2\beta^- \text{M1}$	g.s.	$\geq 1.0(1.4) \times 10^{18}$	
$^{180}\text{W} \rightarrow ^{180}\text{Hf}$	$0\nu 2\varepsilon$	g.s.	$\geq 0.86(1.2) \times 10^{18}$	$\geq 0.9(1.3) \times 10^{17}$ [13]
	$2\nu 2K$	g.s.	$\geq 6.6(9.4) \times 10^{17}$	$\geq 0.7(0.8) \times 10^{17}$ [13]
$^{186}\text{W} \rightarrow ^{186}\text{Os}$	$0\nu 2\beta^-$	g.s.	$\geq 2.1(4.2) \times 10^{20}$	$\geq 1.1(2.1) \times 10^{21}$ [13]
	$0\nu 2\beta^-$	$2^+$ (137.2 keV)	$\geq 2.1(4.2) \times 10^{20}$	$\geq 1.1(2.0) \times 10^{21}$ [13]
	$0\nu 2\beta^- \text{M1}$	g.s.	$\geq 5.8(8.6) \times 10^{19}$	$\geq 1.2(1.4) \times 10^{20}$ [13]
	$2\nu 2\beta^-$	g.s.	$\geq 2.3(2.8) \times 10^{19}$	$\geq 3.7(5.3) \times 10^{18}$ [13]
	$2\nu 2\beta^-$	$2^+$ (137.2 keV)	$\geq 1.8(3.6) \times 10^{20}$	$\geq 1.0(1.3) \times 10^{19}$ [13]

## 5. Conclusions

Low background experiments to search for  $2\beta$  processes in  $^{64}\text{Zn}$ ,  $^{70}\text{Zn}$ ,  $^{180}\text{W}$ ,  $^{186}\text{W}$  were carried out over more than ten thousand hours in the underground Gran Sasso National Laboratories of INFN by using low background large volume (0.1–0.7 kg)  $\text{ZnWO}_4$  crystal scintillators.

New improved half-life limits on double electron capture and electron capture with positron emission in  $^{64}\text{Zn}$  have been set, in particular (all the limits are at 90% C.L.):  $T_{1/2}^{0\nu 2\varepsilon} \geq 1.1 \times 10^{20}$  yr,  $T_{1/2}^{2\nu\varepsilon\beta^+} \geq 7.0 \times 10^{20}$  yr, and  $T_{1/2}^{0\nu\varepsilon\beta^+} \geq 4.3 \times 10^{20}$  yr. The positive indication on the  $(2\nu + 0\nu)\varepsilon\beta^+$  decay of  $^{64}\text{Zn}$  with  $T_{1/2} = (1.1 \pm 0.9) \times 10^{19}$  yr suggested in [8] is completely ruled out by the present experiment. To date only two nuclei ( $^{40}\text{Ca}$  and  $^{78}\text{Kr}$ ) were studied at the similar level of sensitivity. However, it is worth noting that the theoretical predictions are still higher.

The half-life limits on the  $2\beta$  processes in  $^{70}\text{Zn}$ ,  $^{180}\text{W}$ , and the two neutrino mode of  $2\beta$  decay in  $^{186}\text{W}$  established in our work on the level of  $10^{17}$ – $10^{20}$  yr are one order of magnitude higher than those set in previous experiments.

We have found  $\text{ZnWO}_4$  crystal scintillators extremely radiopure detectors with typical contamination at the level of  $\mu\text{Bq/kg}$  ( $^{228}\text{Th}$  and  $^{226}\text{Ra}$ ),  $\leq 0.06$  mBq/kg ( $^{210}\text{Po}$ ), total  $\alpha$  activity (U/Th) 0.2–0.4 mBq/kg,  $\leq 0.4$  mBq/kg ( $^{40}\text{K}$ ),  $\leq 0.05$  mBq/kg ( $^{137}\text{Cs}$ ),  $\leq 0.4$  mBq/kg ( $^{90}\text{Sr}$ – $^{90}\text{Y}$ ),  $\leq 0.01$  mBq/kg ( $^{147}\text{Sm}$ ), and  $\leq 3$  mBq/kg ( $^{87}\text{Rb}$ ).

Further improvements in sensitivity can be reached by increasing the mass of the  $\text{ZnWO}_4$  detector, suppression of external background and development of  $\text{ZnWO}_4$  scintillators with lower level of radioactive contamination. High abundance of  $^{64}\text{Zn}$  (48.3%) allows to build a large scale experiment without expensive isotopical enrichment. An experiment involving  $\approx 10$  tons of *nonenriched* crystals ( $9 \times 10^{27}$  nuclei of  $^{64}\text{Zn}$ ) could reach the half-life sensitivity  $\sim 3 \times 10^{28}$  yr (supposing zero background during ten years of measurements). Such a sensitivity could contribute to our understanding of the neutrino mass mechanism and right-handed currents in neutrinoless processes [5]. The two neutrino double electron capture should be surely observed: in accordance with theoretical expectations [27,28],  $T_{1/2}$  for the  $2\nu 2\varepsilon$  process is predicted on the level of  $10^{25}$ – $10^{26}$  yr.

## Acknowledgements

The group from the Institute for Nuclear Research (Kyiv, Ukraine) was supported in part by the Project “Kosmomikrofizyka” (Astroparticle Physics) of the National Academy of Sciences of Ukraine.

## References

- [1] F.T. Avignone III, S.R. Elliott, J. Engel, Rev. Mod. Phys. 80 (2008) 481;  
H.V. Klapdor-Kleingrothaus, Int. J. Mod. Phys. E 17 (2008) 505;  
H. Ejiri, J. Phys. Soc. Jpn. 74 (2005) 2101;  
F.T. Avignone III, G.S. King, Yu.G. Zdesenko, New J. Phys. 7 (2005) 6;  
S.R. Elliot, J. Engel, J. Phys. G: Nucl. Part. Phys. 30 (2004) R183;  
J.D. Vergados, Phys. Rep. 361 (2002) 1;  
S.R. Elliot, P. Vogel, Annu. Rev. Nucl. Part. Sci. 52 (2002) 115;  
Yu.G. Zdesenko, Rev. Mod. Phys. 74 (2002) 663.
- [2] U. Dore, D. Orestano, Rep. Prog. Phys. 71 (2008) 106201;  
R.N. Mohapatra, et al., Rep. Prog. Phys. 70 (2007) 1757.
- [3] V.I. Tretyak, Yu.G. Zdesenko, At. Data Nucl. Data Tables 61 (1995) 43;  
V.I. Tretyak, Yu.G. Zdesenko, At. Data Nucl. Data Tables 80 (2002) 83.
- [4] A.S. Barabash, Czech. J. Phys. 56 (2006) 437.
- [5] M. Hirsch, et al., Z. Phys. A 347 (1994) 151.
- [6] G. Audi, A.H. Wapstra, C. Thibault, Nucl. Phys. A 729 (2003) 337.
- [7] J.K. Bohlke, et al., J. Phys. Chem. Ref. Data 34 (2005) 57.
- [8] I. Bikit, et al., Appl. Radiat. Isot. 46 (1995) 455.
- [9] H. Kiel, et al., Nucl. Phys. A 723 (2003) 499.
- [10] F.A. Danevich, et al., Nucl. Instrum. Methods A 544 (2005) 553.
- [11] H.J. Kim, et al., Nucl. Phys. A 793 (2007) 171.
- [12] P. Belli, et al., Phys. Lett. B 658 (2008) 193.
- [13] F.A. Danevich, et al., Phys. Rev. C 68 (2003) 035501.
- [14] L.L. Nagornaya, et al., IEEE Trans. Nucl. Sci. 55 (2008) 1469;  
L.L. Nagornaya, et al., Large volume  $\text{ZnWO}_4$  crystal scintillator with excellent energy resolution and low background, presented on 2008 Symposium on Radiation Measurements and Applications (SORMA WEST 2008), 2–5 June 2008, Berkeley, California, USA.
- [15] F.A. Danevich, et al., Phys. Lett. B 344 (1995) 72.
- [16] F.A. Danevich, et al., Nucl. Phys. A 694 (2001) 375.
- [17] E. Gatti, F. De Martini, Nuclear Electronics 2, IAEA, Vienna, 1962, p. 265.
- [18] P. Belli, et al., Nucl. Phys. A 789 (2007) 15.
- [19] S. Agostinelli, et al., Nucl. Instrum. Methods A 506 (2003) 250;  
J. Allison, et al., IEEE Trans. Nucl. Sci. 53 (2006) 270.
- [20] O.A. Ponkratenko, et al., Phys. At. Nucl. 63 (2000) 1282;  
V.I. Tretyak, in preparation.

- [21] R. Bernabei, et al., *Nuovo Cimento A* 112 (1999) 545.
- [22] R.B. Firestone, et al., *Table of Isotopes*, 8th ed., John Wiley, New York, 1996;  
R.B. Firestone et al., CD update, 1998.
- [23] G.J. Feldman, R.D. Cousins, *Phys. Rev. D* 57 (1998) 3873.
- [24] J.D. Vergados, *Nucl. Phys. B* 218 (1983) 109.
- [25] J. Suhonen, M. Aunola, *Nucl. Phys. A* 723 (2003) 271.
- [26] O. Castanos, J.G. Hirsch, O. Civitarese, P.O. Hess, *Nucl. Phys. A* 571 (1994) 276.
- [27] P. Domin, S. Kovalenko, F. Simkovic, S.V. Semenov, *Nucl. Phys. A* 753 (2005) 337.
- [28] E.-W. Grewe, et al., *Phys. Rev. C* 77 (2008) 064303.